

## Fluorescence labelling

E.M. GOLDYS<sup>1</sup>, K. DROZDOWICZ-TOMSIA<sup>1</sup>, G. ZHU<sup>1</sup>, H. YU<sup>1</sup>, S. JINJUN<sup>1</sup>,  
M. MOTLAN<sup>1</sup>, M. GODLEWSKI<sup>2</sup>

<sup>1</sup>Macquarie University Biotechnology Research Institute, Macquarie University,  
Sydney 2109 NSW, Australia

<sup>2</sup>Institute of Physics Polish Academy of Sciences, al. Lotników 32/46, 02-668 Warsaw, Poland

Fluorescence labelling has become a technique of increasing importance in modern biotechnology which is increasingly underpinned by advances in materials science. In this paper we describe our contributions to this area. In order to expand the understanding of *in vivo* fluorescence labelling we carried out the staining of membrane-based structures in effectively secreting *Trichoderma reesei* using the fluorescent dye FM 4-64 and their confocal microscopy studies. We also describe the observation of efficient fluorescence upconversion in Sm-doped Gd<sub>2</sub>O<sub>3</sub> nanopowders synthesised by the spray pyrolysis method. This result indicates the potential for Sm-doped Gd<sub>2</sub>O<sub>3</sub> to perform as a fluorescent label excited in red, yellow and green and emitting in blue. Finally, we report a simple approach for synthesizing water-soluble CdS nanoparticles by using ethylenediaminetetraacetic acid disodium salt dihydrate (EDTA) as a stabilizer.

Keywords: fluorescence labelling, europium doped Gd<sub>2</sub>O<sub>3</sub>, samarium doped Gd<sub>2</sub>O<sub>3</sub>, upconversion, cadmium sulfide nanoparticles.

### 1. Introduction to fluorescence labelling

The technique of fluorescence labelling has revolutionized modern life sciences. Fluorescent molecules or nanoparticles can be designed to bind with biological macromolecules where they offer scope for quantitative analysis of biochemical reactions. Many fluorescent dyes localise within specific organelles including cytoskeleton, mitochondria, Golgi apparatus, endoplasmic reticulum and nucleus making it possible to establish a detailed picture of cellular environment and its processes. Thanks to environmental sensitivity the fluorescent labels can be used to monitor dynamic processes and localised environmental variables such as: concentration of metallic ions, pH, reactive oxygen species, membrane potential. A significant body of work exists concerning monitoring of cellular integrity, endocytosis, exocytosis, membrane fluidity, protein trafficking, signal transduction and enzymatic activity. Finally, through advanced fluorescent assays and technologies such as gene chips, fluorescent labels facilitate genetic mapping and chromosome analysis in molecular genetics.

It is worthwhile to establish the length scales relevant for biological labelling. Small dye molecules such as fluorescein (FITC) are about 1 nm in size. Fluorescent proteins such as green fluorescent protein (GFP) and its variants, that play a crucial role in modern biology because they can be genetically targeted, are around 10 nm in size. A typical bacterial cell is about 1 micrometer in diameter, while animal cells typically range from several micrometers to few tens of nm, but some can be much larger. These relationships emphasise that fluorescent labelling is well suited for most biological applications.

A wide variety of fluorescent molecules are now available for fluorescent labelling, and catalogues of companies such as Invitrogen list a very broad range of fluorophores to suit most applications. They are often characterized by high quantum efficiencies, but most molecular probes suffer from a narrow optimum excitation region, relative proximity of the excitation and emission regions being very close, relatively broad emission limiting their applicability as multiple labels and sensitivity to photobleaching. In response to these concerns semiconductor quantum dots (QD) have been developed. Most of the QDs available commercially are II-VI nanocrystals, whose optical properties are dictated by quantum confinement. Their spectrally narrow emission characteristics are accompanied by high brightness comparable to fluorescent dyes and the ability to excite multiple colours with a single excitation wavelength. The latter is their unique feature, beneficial for multiple labelling.

The semiconductor QDs presently used are mostly core-shell structures with the core of one II-VI material and the shell from another, often with higher bandgap, such as CdSe/ZnS pair. In order to be used for fluorescent labelling the QDs must be made water soluble and able to be conjugated to biomolecules. An ultrathin polymer layer and a covalently attached outer layer of streptavidin ensure easy access to chemical groups that facilitate binding. The final size of the QD is in the order of 10–15 nm, which is comparatively large with respect to the size of pores in cellular membranes. Consequently, applications of QDs in fluorescent labelling as detection reagents in microscopy must rely on special strategies to introduce these large objects to the cells. Such strategies sometimes exploit the internal cellular transport mechanisms. Other applications of QDs, for example, in DNA chips, flow cytometry and immunoassays experience less constraints and rapid progress is being made. QDs and QD-encoded beads are presently used as platforms for highly multiplexed assays in proteomics, genotyping and gene expression. Future applications for *in vivo* imaging not only in cells but also in tissues and living organisms are also under development.

Our research program is concerned with lanthanide doped nanocrystals. Lanthanide ions confer significant advantages to semiconductor nanoparticles that are important for fluorescence labelling. They offer the potential for multi-colour imaging with single wavelength excitation by using different ions. As with all lanthanides upconversion processes can be expected with excitation in NIR and the emission in visible. The NIR excitation offers deeper penetration into tissues and helps eliminate background luminescence. Additionally, upconversion offers higher efficiency than the multiphoton excitation. The lanthanide ions have comparatively long lifetime,

useful for time-resolved methods and photobleaching important in fluorescent molecules should be strongly reduced.

We are reporting here our preliminary studies of *in vivo* fluorescent labelling which we carried out in the context of a systems biology program to map out the secretion pathway in a cell. Further we present the results of spectroscopic and laser scanning microscopy investigations of lanthanide doped nanoparticles. Finally, we present the preliminary studies of bulk wet chemical synthesis of such nanoparticles. The paper is divided into three sections describing these three groups of results.

## 2. *In vivo* fluorescence labelling using chemical dyes – tagging of membranes and selected organelles in the living fungus *Trichoderma reesei*

*Trichoderma reesei* is an industrially important microorganism that is able to secrete abundant quantities of native enzymes, in the order of grams per litre. The fungus can be genetically engineered to secrete valuable gene products such as growth factors, however at much lower yields, due to unidentified secretion roadblocks [1]. In order to be able to trace the secretion of endogenous and foreign proteins through secretory pathways they need to be visualized using fluorescent labelling.

FM 4-64 is one of amphiphilic styryl dyes whose properties are described at <http://www.probes.com>. We used FM 4-64 to visualize secretory pathways because it is membrane selective, compatible with fluorescent proteins (GFP/YFP) used in fluorescence resonance energy transfer (FRET) experiments, and it has also other advantages such as photostability and low-toxicity [2].

We examined the spectral characteristics of FM 4-64 in *T. reesei*, shown in Fig. 1. The dye in the living fungus shows the emission extending in the range 560 to 720 nm, with the maximum at 646 nm. The red curve shows the solution of the same dye in

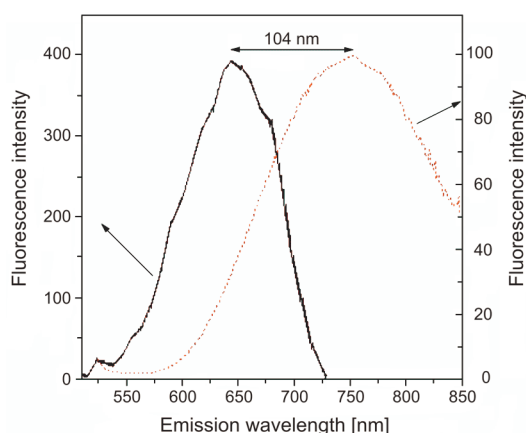


Fig. 1. Fluorescence of FM 4-64 in *T. reesei* cells (left curve). Right curve shows the spectrum of a pure dye solution in methanol. The spectral shift is due to the effect of cellular environment.

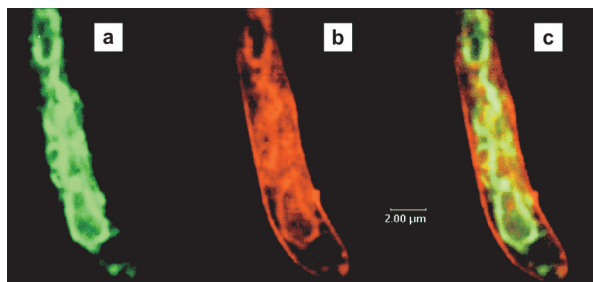


Fig. 2. Fluorescence staining with FM 4-64 and BODIPY FL C5: staining with BODIPY FL C5 (a); FM 4-64 (b). The overlapped image (c) with yellow color marking shows co-localization.

methanol, which is spectrally shifted by 104 nm towards longer wavelength. Such large shift is due to the effect of cellular environment on the dye molecules. It should be emphasized that this spectral characteristic is very different from GFP and RFP [3] and thus FM 4-64 can be used in *T. reesei* in conjunction with genetically targeted probes.

We also explored the time evolution of staining with FM 4-64. The intensity of staining progressively increases over a course of about 150 minutes and approaches saturation after that. Further we explored double labelling with organelle-specific dyes in *T. reesei*. Three dyes were used in this study, these were an endoplasmic reticulum (ER) dye DIOC6(3), a Golgi dye BODIPY FL C5 and a nucleus stain SYTO 40. These data are presented in Fig. 2. We observe that apart from the nucleus stain SYTO 40, none of applied staining seemed to be specific to single organelles in *T. reesei*.

### 3. Spectral properties of $Gd_2O_3:Sm$ and $Gd_2O_3:Eu$ doped nanoparticles and their potential for fluorescence labelling

The  $Gd_2O_3$  nanoparticles examined in this study were produced by spray pyrolysis method [4], a simple technology that provides excellent doping control. The nanoparticles were doped with 10% Sm and 10% Eu and they showed fluorescence emission at a range of excitation wavelengths. Selected excitation and emission spectra for  $Gd_2O_3$  (with the emission excited at 405 nm and excitation detected at 603 nm) are presented in Fig. 3. The spectra show a range of peaks that have been attributed to specific transitions within Sm shown in Fig. 4 [5–11]. A comparative set of data for Eu-doped nanoparticles is presented in Fig. 5. In both excitation curves for Sm and Eu we observe a broad excitation band, in contrast to bulk rare earth doped materials, where the excitation curve is composed of single isolated lines corresponding to appropriate transitions. In both types of nanoparticles we observe these transitions on a broad and intense background, which indicates that rare earth ions in nanoparticles can be excited using a broad variety of excitation wavelengths.

The results presented in Figs. 3 and 5 were taken using a fluorimeter with Xe lamp excitation at a spectral resolution of 2 nm in emission and 5 nm in excitation. The same

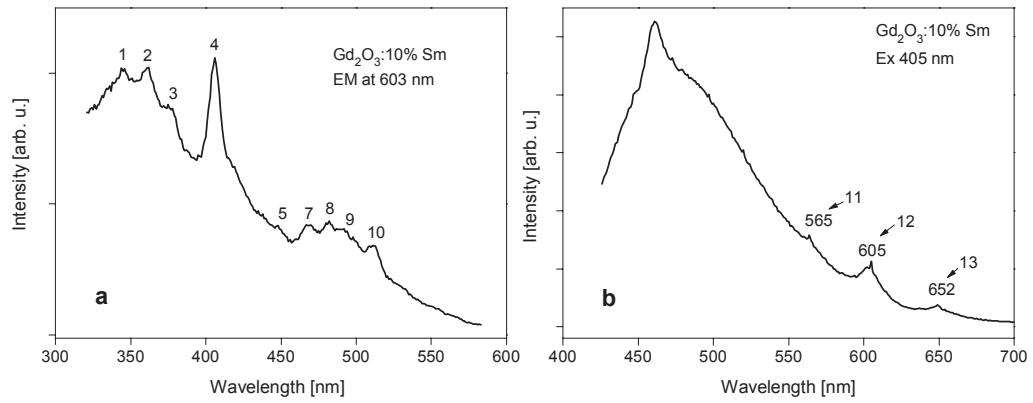


Fig. 3. Selected excitation (a) and emission (b) spectra for  $Gd_2O_3$  doped with 10% Sm. The emission is excited at 405 nm and excitation detected at 603 nm.

nanoparticles were examined using a laser scanning microscope Leica TCS SP2 with full spectral capabilities. The excitation wavelength used in these studies was 405 nm, the same as previously, and the spectral resolution was 5 nm. The main Sm and Eu lines were clearly visible under these conditions (data not shown).

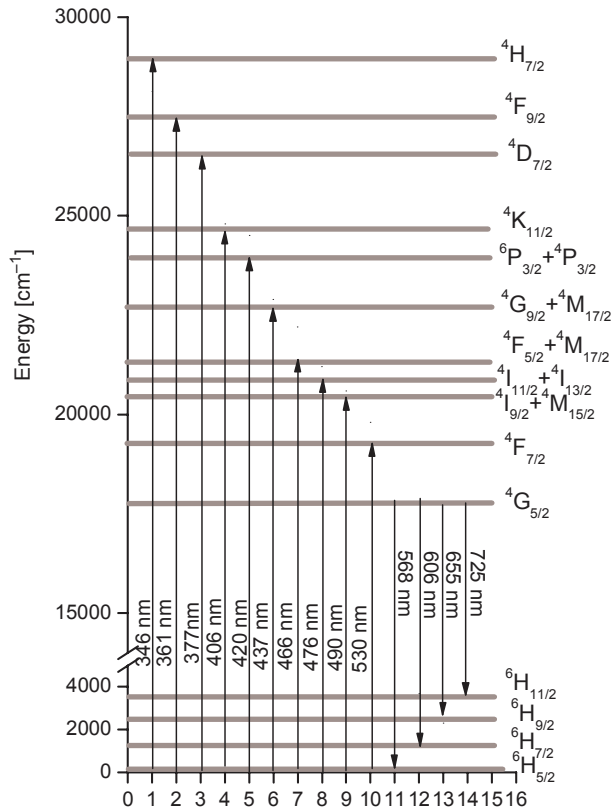


Fig. 4. Schematic diagram of transitions in  $Sm^{3+}$ .

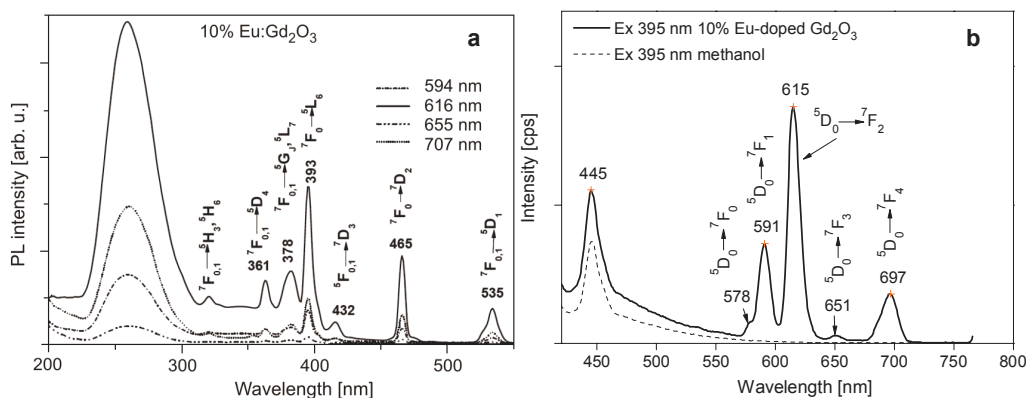


Fig. 5. Selected excitation (a) and emission (b) spectra for Gd<sub>2</sub>O<sub>3</sub> doped with 20% Eu. The emission is excited at 405 nm and excitation detected at 614 nm.

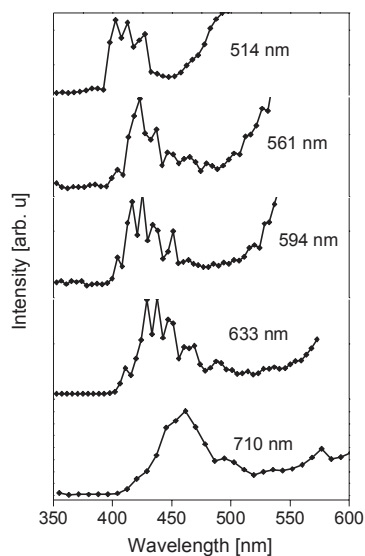


Fig. 6. Fluorescence up-conversion for excitation at 514, 561, 594, 633 and 710 nm.

Further we explored the spectral properties of these nanoparticles with varying excitation wavelengths in a laser scanning microscope. The results presented here were taken for a Sm-doped sample excited at 710, 633, 594, 561 and 514 nm. We observed a clear fluorescence upconversion, in the form of a blue band that shifted with excitation energy (Fig. 6). The emission takes place at shorter wavelengths when excited at 514 nm and moves towards longer wavelengths with 710 nm excitation. These nanoparticles have also been functionalised [12] and used for fluorescence labelling studies of human lymphoma cells.

#### 4. Synthesis of CdS nanoparticles in the presence of Eu and EDTA

In an effort to produce larger quantities of rare earth doped nanoparticles we attempted their wet chemical synthesis method following reference [13]. It should be noted that large difference in size of host cation and lanthanide ions, charge mismatch between the cations, different coordination numbers in crystallographic structures, and low affinity of lanthanide ions towards sulfur and selenium make it difficult to achieve doping inside of the nanoparticles. We have therefore explored the synthesis of II-VI nanoparticles with a capping layer capable of binding RE ions. Our approach was to use ethylenediaminetetraacetic acid disodium salt dihydrate (EDTA) both as a capping agent for synthesis of CdS nanoparticles and a ligand forming complex with  $\text{Eu}^{3+}$  in non-coordinating solvent ethylene glycol [13].

In the procedure, 532 mg  $\text{CdAc}_2 \cdot 2\text{H}_2\text{O}$  is dissolved in 100 ml ethylene glycol (EG) solution at room temperature (solution 1); 78 mg thiourea and 372 mg EDTA are separately dissolved in another 100 ml EG solution at  $120^\circ\text{C}$  (solution 2). Under vigorous magnetic stirring, the solution 2 is quickly injected to the solution 1. The mixed solution is clear until it is heated to the EG's boiling point ( $200^\circ\text{C}$ ); then after about 10 min the solution became milky yellow, indicating the formation of CdS nanoparticles.

The synthesis with addition of EDTA leads to better control of nanoparticle size and agglomeration, but still leads to formation of nanoparticles with broad size distribution and vacancy sulphur defect dominated fluorescence.

Fluorescence of CdS and CdS capped with Eu-EDTA complex nanoparticles is shown in Fig. 7. It is clear that CdS EDTA capped nanoparticles without  $\text{Eu}^{3+}$  show much weaker fluorescence, dominated by the surface and vacancy sulphur defects. The formation of EDTA–Eu complex increases band gap fluorescence of CdS. No energy transfer between NPs and RE ion was observed. This work is a preliminary

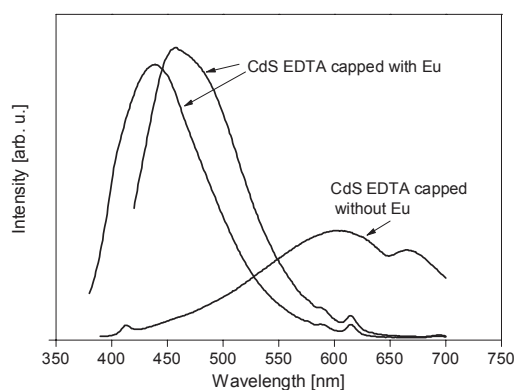


Fig. 7. Fluorescence of CdS and CdS capped with Eu-EDTA complex nanoparticles excited at 405 nm.

step towards the modification of the established method where the TOPO capping layer is formed on CdSe nanoparticles with ability to form complexes with RE.

In summary we described here our results of organelle-specific staining using chemical dyes in *T. reesei*, and current status of projects on upconversion and fluorescence labelling using rare earth doped Gd<sub>2</sub>O<sub>3</sub> nanoparticles as well as novel approaches to wet synthesis of rare earth doped II-VI nanoparticles.

## References

- [1] NEVALAINEN K.M.H., TE'O V.S.J., [In] *Applied Mycology and Biotechnology*, [Eds.] D.K. Arora, G.G. Khachatourians, Vol. 3, 2003, pp. 241–59.
- [2] READ N.D., HICKEY P.C., [In] *Vol 328 NATO Science Series: Cell biology of plant and fungal tip growth*, [Eds.] A. Geitmann, M. Cresti, I.B. Heath, IOS Press, Amsterdam 2001, pp. 137–48.
- [3] CHALFIE M., TU Y., EUSKIRCHEN G., WARD W.W., PRASHER D.C., *Green fluorescent protein as a marker for gene expression*, *Science* **263**(5148), 1994, pp. 802–5.
- [4] DOSEV D., NICHKOVA M., LIU M., GUO B., LIU G., XIA Y., HAMMOCK B.D., KENNEDY I.M., *Application of fluorescent Eu:Gd<sub>2</sub>O<sub>3</sub> nanoparticles to the visualization of protein micropatterns*, *Proceedings of SPIE* **5699**, 2005, pp. 473–81.
- [5] TREADAWAY M.J., POWELL R.C., *Energy transfer in samarian-doped calcium tungstate crystals*, *Physical Review B: Solid State* **11**(2), 1975, pp. 862–74.
- [6] ZHOU Y., LIN J., WANG S., *Energy transfer and upconversion luminescence properties of Y<sub>2</sub>O<sub>3</sub>:Sm and Gd<sub>2</sub>O<sub>3</sub>:Sm phosphors*, *Journal of Solid State Chemistry* **171**(1–2), 2003, pp. 391–5.
- [7] AREVA S., HOLSÁ J., LAMMINMAKI R.-J., RAHIALA H., DEREN P., STREK W., *Excited state absorption processes in Sm<sup>3+</sup> doped GdOCl*, *Journal of Alloys and Compounds* **300–301**, 2000, pp. 218–23.
- [8] STEVENS S.B., MORRISON C.A., SELTZER M.D., HILLS M.E., GRUBER J.B., *Emission measurements and crystal-field calculations for <sup>4</sup>G<sub>5/2</sub> to <sup>6</sup>H<sub>7/2</sub> transitions in Sm<sup>3+</sup>:YAG*, *Journal of Applied Physics* **70**(2), 1991, pp. 948–53.
- [9] DE LA ROSA-CRUZ E., DIAZ-TORRES L.A., SALAS P., RODRIGUEZ R.A., KUMAR G.A., MENESES M.A., MOSINO J.F., HERNANDEZ J.M., BARBOSA-GARCIA O., *Luminescent properties and energy transfer in ZrO<sub>2</sub>:Sm<sup>3+</sup> nanocrystals*, *Journal of Applied Physics* **94**(5), 2003, pp. 3509–15.
- [10] BIJU P.R., JOSE G., THOMAS V., NAMPOORI V.P.N., UNNIKRISHNAN N.V., *Energy transfer in Sm<sup>3+</sup>:Eu<sup>3+</sup> system in zinc sodium phosphate glasses*, *Optical Materials* **24**(4), 2004, pp. 671–7.
- [11] MARTINEZ-SANCHEZ E., GARCIA-HIPOLITO M., GUZMAN J., RAMOS-BRITO F., SANTOYO-SALAZAR J., MARTINEZ-MARTINEZ R., ALVAREZ-FREGOSO O., RAMOS-CORTES M.I., MENDEZ-DELGADO J.J., FALCONY C., *Cathodoluminescent characteristics of Sm-doped ZnAl<sub>2</sub>O<sub>4</sub> nanostructured powders*, *Physica Status Solidi A* **202**(1), 2005, pp. 102–7.
- [12] DOSEV D., NICHKOVA M., GODLEWSKI M., TOMSIA K., GRYCZYNSKI I., GOLDYS E.M., KENNEDY I.M., *6th International Weber Symposium on Innovative Fluorescence Methodologies in Biochemistry and Medicine*, Kauai, Hawaii, July 22–28, 2005.
- [13] ZHAO Y., ZHANG Y., ZHU H., HADJIPANAYIS G.C., XIAO J.Q., *Low-temperature synthesis of hexagonal (wurtzite) ZnS nanocrystals*, *Journal of the American Chemical Society* **126**(22), 2004, pp. 6874–5.

*Received December 15, 2005*